Article

Not peer-reviewed version

Novel Anti-melanoma Leads Are Efficacious in A375 Cell Line Xenograft Melanoma Model in Nude Mice

Sadeeshkumar Velayutham , Ryan Seerattan , Maab Sultan , Trisha Seal , Samaya Danthurthy , Baskaran Chinnapan , Jessica Landi , Kaitlyn Pearl , Aveta Singh , Keiran S.M. Smalley , Julia Zaias , Jun Yong Choi , Dmitriy Minond *

Posted Date: 15 May 2023

doi: 10.20944/preprints202305.1006.v1

Keywords: Melanoma; drug discovery; spliceosomal inhibition; BRAF; cell line xenograft; organ histopathology

Article

Novel Anti-Melanoma Leads Are Efficacious in A375 Cell Line Xenograft Melanoma Model in Nude Mice

Sadeeshkumar Velayutham [1,2], Ryan Seerattan [3], Maab Sultan [2], Trisha Seal [4], Samaya Danthurthy [5], Baskaran Chinnappan [1,2], Jessica Landi [6], Kaitlyn Pearl [6], Aveta Singh [3], Keiran S.M. Smalley [7], Julia Zaias [8], Jun Yong Choi [3,9,*,†] and Dmitriy Minond [1,2,*,†]

[1] College of Pharmacy, Nova Southeastern University, 3321 College Avenue, Fort Lauderdale, FL 33314.
[2] Rumbaugh-Goodwin Institute for Cancer Research, Nova Southeastern University, 3321 College Avenue, CCR r.605, Fort Lauderdale, FL 33314.
[3] Department of Chemistry and Biochemistry, Queens College, 65-30 Kissena Boulevard, Flushing, NY 11367
[4] Halmos College of Arts and Sciences, Nova Southeastern University, 3301 College Avenue, Fort Lauderdale, FL 33314.
[5] Honors College, Nova Southeastern University, 8000 N Ocean Dr, Dania Beach, FL 33004.
[6] Dr. Kiran C. Patel College of Osteopathic Medicine, Nova Southeastern University, 3321 College Avenue, Fort Lauderdale, FL 33314.
[7] Department of Tumor Biology, Moffitt Cancer Center, 12902 Magnolia Drive, Tampa, FL 33612.
[8] University of Miami, Division of Comparative Pathology, 1501 NW 10th Ave, Miami, FL 33136
[9] Ph.D. Programs in Chemistry and Biochemistry, The Graduate Center of the City University of New York, 365 5th Ave, New York, NY 10016
* Correspondence: dminond@nova.edu; junyong.choi@qc.cuny.edu
† These authors share senior authorship.

Abstract: Despite the recent advances in melanoma therapy, the need for new targets and novel approaches to therapy is urgent. We previously reported melanoma actives that work *via* binding and downregulating spliceosomal proteins hnRNPH1 and H2. In a separate study, we reported that these compounds were non-toxic to Balb/C mice at 50 mg/kg suggesting their utility in in vivo studies. In the present study, we aimed to determine the therapeutic potential of these compounds by testing them in A375 cell-line derived xenograft in nu/nu mice. Animals were randomized into four groups (n=12/group) to receive subcutaneous administration of vehicle, 10 mg/kg vemurafenib, and 25 mg/kg 2155-14 and 2155-18 three times per week for 15 days along with a control group. The results revealed that both 2155-14 and 2155-18 significantly decreased the growth of A375 tumors, which was comparable to vemurafenib. These results were confirmed by tumor volume, weight, and histopathological examination. In conclusion, these results suggest a therapeutic potential of targeting spliceosomal proteins hnRNPH1 and H2.

Keywords: melanoma; drug discovery; spliceosomal inhibition; BRAF; cell line xenograft; organ histopathology

1. Introduction

Melanoma is the deadliest form of skin cancer responsible for more than 7,000 deaths a year in US alone (1). Before approval of immunotherapy, melanoma patients with metastatic disease had a 5-year survival rate of approximately 20% (2). Immunotherapy alone or combination with small molecule drugs improved overall 5-year survival (OS) to 50% with approximately 40% of patients responding to the therapy (3, 4). However, adverse effects to immunotherapy, especially the combination of anti-CTL-4 and anti-PD-1 treatment, often lead to the stoppage of the treatment (5, 6). Additionally, a portion of the patients who initially respond to the therapy eventually acquire resistance (7). Based on these considerations novel approaches to melanoma therapy are needed.

We previously reported the discovery of spliceosome-binding small molecules active against melanoma in vitro (8, 9) and non-toxic to mice (10). We demonstrated that mechanism of action of these molecules is based on binding of hnRNP H1 and H2 which are RNA-binding proteins (RBPs)

 doi:10.20944/preprints202305.1006.v1

with the role in pre-mRNA splicing (11). RBPs have attracted attention as targets for cancer drug discovery due to being differentially expressed in many cancers (12). There have been multiple reports of RBP inhibitors (RBPIs) targeting various RBPs (12). Several small molecules targeting eIF4A have been reported by others. Most pertinent to the present study, DMDA-Pat A, a structural analogue of the marine natural product pateamine A, demonstrated in vivo activity against MDA-MB-435 cell-derived melanoma xenograft (CDX) at 0.9 mg/kg bw in mice (13). Small molecule 4EGI-1, an inhibitor of RBP eIF4E/G with Ki of 25 μM, inhibited growth of CRL-2813 melanoma mouse CDX at 25 and 75 mg/kg q.d. (14). Remarkably, neither inhibitor exhibited overt toxicity at the tested doses.

Both eIF4A and eIF4E/G are involved in mRNA translation, however, there are examples of small molecules targeting other RNA-related processes. Small molecules E7107, Spliceostatin A, and H3B-8800 target mRNA splicing by modulating Splicing Factor 3B1 (SF3B1). E7107 demonstrated efficacy in a pre-clinical model of NSCLC at 20 mg/kg; however, it exhibited dose-dependent toxicity in two Phase I clinical trials (15, 16) (MTD = 4mg/m^2) which led to the discontinuation of this trial. H3B-8800 treatment was associated with mostly low-grade adverse effects after 1-40 mg once-daily dose (17) in Phase I trial in patients with myelodysplastic syndromes (MDS), chronic myelomonocytic leukemia (CMML), and secondary acute myeloid leukemia (AML) arising from MDS.

In the present study we tested efficacy of two small molecules that bind and downregulate spliceosomal proteins hnRNP H1 and H2 in a cell-derived xenograft mouse model of BRAF-mutant melanoma.

2. Materials and Methods

Procedure for the synthesis of 2155-14 (JC-395) and 2155-18 (JC-408). Pyrrolidine-bis-diketopiperazine JC-395 and JC-408 (Figure 1A) were synthesized by modifying the previously published method (9). Both compounds were synthesized via solid-phase methodology (Scheme 1) on 4-methylbenzhydrylamine hydrochloride resin (MBHA) (1.4 mmol/g, 100-200 mesh). To a syringe with a solid filter at the bottom was added MBHA resin (150 mg, 1 eq.), which was swelled and neutralized using 10% diisopropylethylamine (DIEA)/dimethylformamide (DMF) (v/v) (4 mL) at 25 °C for 20 min. After draining the swelling solution, the resin was washed with DCM (2x), Methanol (2x), DMF (2x), then DCM (2x). [Coupling reaction with amino acid] To an empty glass vial were added Boc-protected amino acid (Boc-Phe-OH, 4 eq.), 1-[Bis(dimethylamino)methylene]-1H-1,2,3-triazolo[4,5-b]pyridinium 3-oxide hexafluorophosphate (HATU, 4 eq.), and hydroxybenzotriazole hydrate (HOBt, 4 eq), and 10% DIEA/DMF was added to the mixture, which was shaken for 15 min for pre-activation. The pre-activated solution was added to the syringe containing the neutralized resin, and the syringe was shaken for 4 h at 25 °C. The solution was drained from the syringe, and the resin was washed with DCM (2x), Methanol (2x), DMF (2x), and DCM (2x). Around 10-15 beads of resin were taken for the Kaiser test. [Boc deprotection and neutralization] Boc protecting groups were removed with 55% trifluoroacetic acid (TFA)/45% dichloromethane (DCM) (1x, 4 mL, 30 min) and subsequently neutralized with 10% diisopropylethylamine (DIEA)/90% DCM (3x, 5 min). The steps for the coupling reaction with amino acid, Boc-deprotection, and neutralization were repeated with different amino acids such as Boc-Pro-OH, Boc-β-cyclohexyl-D-alanine-OH (or Boc-Phe-OH for JC-408), and Fmoc-Tyr(OtBu)-OH in sequence: the reaction time for coupling with amino acids was 2 h. The terminal Fmoc group was deprotected with 20% piperidine in DMF (4 mL) by shaking at 25 °C for 30 min. After drain the solution and wash the resin with DCM (2x), Methanol (2x), DMF (2x), then DCM (2x), phenylacetic acid (4 eq.) or 2-(Adamantan-1-yl)acetic acid (4 eq.) for compound 18, HATU, (4 eq.), HOBt (4 eq.) in 10%DIEA/90%DMF (4 ml) were pre-activated in a glass vial for 15 min and added to the syringe for shaking at 25 °C for 2 h. After the washing step, the resin was transferred to a microwave vial, and Borane-THF (1M, 6 mL, ~30 eq.) was added to the vial. The reaction mixture was heated under microwave irradiation at 70 °C for 6 h, and the solution was poured off. Piperidine (6 mL) was added to the microwave vial containing the resin, which was heated under microwave irradiation at 70 °C for 30 min. Piperidine was poured off, and the resin was transferred to a clean syringe, which was washed with DCM (2x), Methanol (2x), DMF (2x), then DCM (2x).

 doi:10.20944/preprints202305.1006.v1

Diketopiperazine cyclization was performed under anhydrous conditions. The resin in the syringe was placed in a pressure relief scintillation vial and a solution of 1,1'-oxalyldiimidazole (5x for each cyclization site) in anhydrous DMF (4 mL) was added to the vial, which was stirred at 25 °C for 48 h. After draining the solution, the resin was washed with DCM (2x), Methanol (2x), DMF (2x), then DCM (2x). Completion of cyclization was checked by cleaving a control sample, which was analyzed by LC. The compounds were then cleaved from the resin with trifluoroacetic acid (TFA)/trifluoromethanesulfonic acid (TFMSA) (9:1, 4 mL). The cleavage solution was collected and removed by blowing out N_2 gas. The crude samples were diluted with MeOH (4 mL) and filtered for HPLC purification as described below to produce the title compound (JC-395 or JC-408) as a white powdery solid with 98% or 99% purity, respectively. 1H NMR and Mass spectroscopic data were matched with those in previous report (9).

Compound purification and characterization. The final compounds were purified using preparative HPLC with a dual pump Shimadzu LC-20AP system equipped with a SunFire C18 preparative column (19 x 250 mm, 10 micron) at λ = 220 nm, with a mobile phase of (A) H_2O (0.1% TFA)/(B) methanol (MeOH)/acetonitrile (ACN) (3:1) (0.1% TFA), at a flow rate of 60 mL/min with 10%(B) for 30 sec, a gradient up to 90%(B) for 9.5 min, and 90%(B) for 3 min. ^{1}H NMR and ^{13}C NMR spectra were recorded in DMSO-d_6 on a Bruker Ascend 400 MHz spectrometer at 400.14 and 100.62 MHz, respectively, and mass spectra were recorded using an Advion Mass Express. The purities of the synthesized compounds were confirmed to be greater than 95% by liquid chromatography on a Shimadzu LC-20AD instrument with SPD-20A. The mobile phase of (A) H_2O (0.1% formic acid)/(B) ACN (0.1% formic acid) was used with a gradient of 5-95% over 7 min followed by 3 min rinse and 3 min equilibration.

Animal protocol. This study used 5- to 7-week-old male and female athymic Nu/Nu mice (The Jackson Laboratory, Bar Harbor. ME). The mice were housed in the standard mouse shoe-box cages and maintained in a 12-hr light/12-hr dark cycle, with 50% humidity and 20 ± 3°C. The mice had free access to a standard pellet diet (Certified PicoLab® Rodent Diet 20, Lab Diet) and water *ad libitum*. The study was conducted in accordance with the guidelines of the Nova Southeastern University (NSU) Institutional Animal Care and Use Committee (NSU IACUC protocol 2019.12.DM4).

The animals were allowed to acclimate after delivery. The animals were randomly divided into 5 groups with each group containing 12 mice (6 male and 6 female). Group 1: non-tumor control mice; Group 2: animals were treated with a vehicle control (10%/90% DMSO/sterile water, USP sterile injectable grade); Group 3: animals were treated with vemurafenib (10 mg/kg body weight); Group 4: animals were treated with 2155-14 (25 mg/kg body weight); Group 5: animals were treated with 2155-18 (25 mg/kg body weight) three times/week.

To establish a cell line-derived xenograft (CDX), A375 (ATCC® CRL-1619, ATCC, Manassas, MD, USA) cells were cultured in DMEM media supplemented with 10% FBS, 1% Pen/Strep. On the day of a xenograft implantation, the cells were harvested at 70-80% confluency and suspended in 10 ml of sterile PBS (USP grade, sterile for injection) so that 200 µl contained the required number of cells per injection and kept on ice. 2.0 x 10^6 cells/0.2mL were injected into the right flanks of appropriate groups of mice using 1 ml insulin syringes with 26-gauge needles.

Mice injected with A375 cells were palpated every day to detect the tumor growth. Once tumors were palpable, the digital caliper was used to measure the width and length of the tumors. Tumor volumes were calculated using the Equation 1:

$$\text{Volume} = (\text{width})^2 \times \text{length}/2$$

Compounds (vemurafenib, 2155-14, and 2155-18) were prepared in 10% DMSO/H_2O (both USP injectable grade) fresh for each treatment day. Vemurafenib, 2155-14, and 2155-18 2155-14 and 2155-18 were weighed into autoclaved 1.5 mL Eppendorf vials using analytical scales. USP grade DMSO was added to each vial under aseptic conditions and vortexed. USP grade injectable sterile H_2O was then added to each vial and again vortexed. 1 ml insulin syringes with a 26-gauge needle were filled with 0.2 mL of the compound and delivered to the vivarium in the closed carrier for animal treatment. For the vehicle control group, syringes were filled with 0.2 mL of 10% DMSO/H_2O (USP injectable grade).

Preprints (www.preprints.org) | NOT PEER-REVIEWED | Posted: 15 May 2023 doi:10.20944/preprints202305.1006.v1

During the experimental period, body weights were measured, and mice were observed for signs of clinical distress every day. More specifically, mice were observed for posture, vocalization, ease of handling, lacrimation, chromodacryorrhea, salivation, coat condition, unsupported rearing, arousal, piloerection, motor movements, diarrhea, tail pinch reaction, and constipation.

When tumors reached 2,000 mm^3, the mice were euthanized, tumors excised, weighed, and their volumes were measured again.

The excised tumors were placed in either 10% neutral buffered formalin for paraffin embedding or in -80°C for cryo sectioning for tumor histopathology. The tissues were processed *via* standard tissue processing to produce H&E slides. All H&E slides were reviewed blind to the treatment group. The tumors have also been fluorescently stained for cleaved caspase 3 to detect apoptosis, Ki67 for proliferation, and hnRNPH1/H2 to confirm target modulation. The histopathology analyses were performed at the Division of Comparative Pathology, University of Miami.

Statistical significance was set at $p < 0.05$. All data were analyzed using one-way ANOVA to compare means, and significant differences were further analyzed by Tukey's multiple comparisons using Prism (version 8.0, GraphPad Inc, San Diego, CA).

hnRNP H staining. Tissue sections stored at -80°C were thawed and fixed for 10 min in 4% paraformaldehyde on ice. Samples were washed in PBS and incubated overnight in 30% sucrose in PBS at 4°C. Dissected tissue samples were embedded in Tissue-Tek optimal cutting temperature (OCT) compound (Sakura 4583) and stored at -80°C. Sections of 10µm thickness were cut using the Leica CM1850 UV Cryostat. Sections were washed in PBS for 10 min at RT, Sections treated with 0.1% sodium borohydride in PBS for 10 min, permeabilized in 0.3% Triton X-100 in PBS for 5min at RT and washed in 0.1% Tween20 in TBS. Sections were incubated in blocking buffer (1%BSA, 10% Goat serum, 0.3% triton X100 in PBS) for 1h at RT. The primary antibody for hnRNP H (rabbit monoclonal, 1:250, abcam ab289974) was incubated overnight at 4°C in antibody diluent. Sections were washed three times using 0.1% Tween20 in PBS at RT and incubated with secondary antibody (goat anti-rabbit IgG conjugated to Alexa Fluor 647 (ab150079, abcam) diluted 1:400 in antibody diluent for 1h at RT. Sections were washed three times for 5 min at RT in PBS and mounted in VECTASHIELD Antifade Mounting Medium with DAPI for fluorescence (VECTOR). Images were taken using Evos (Life Technologies) automated microscope.

Sections were stored short term at -20°C and stained with hematoxylin and eosin (H&E, VWR US Cat. No. 95057-844 and VWR US Cat. No. 95057-848) for histopathological examination.

Caspase 3 staining. Tissue samples were dissected and fixed in 4% paraformaldehyde at RT. Once fixed, the tissues were processed overnight on the Leica ASP 300S Processor (Leica Biosystems, GmbH, Germany) and embedded in paraffin. Slides were sectioned at 5µm and stained using the Leica Bond RXm automated research stainer (Leica Biosystems, GmbH, Germany). Slides were baked (60°C), deparaffinized (BOND Dewax deparaffinization solution), underwent epitope retrieval (BOND Epitope Retrieval Solution 1), stained with Anti-Ki67 (Cell Signaling cat# 9664S, 1:200) in combination with the BOND Polymer Refine HRP Plex Detection kit (Leica cat# DS9914), and counterstained with hematoxylin.

Ki67 staining. Tissue samples were dissected and fixed in 4% paraformaldehyde at RT. Once fixed, the tissues were processed overnight on the Leica ASP 300S Processor (Leica Biosystems, GmbH, Germany) and embedded in paraffin. Slides were sectioned at 5µm and stained using the Leica Bond RXm automated research stainer (Leica Biosystems, GmbH, Germany). Slides were baked (60°C), deparaffinized (BOND Dewax deparaffinization solution), underwent epitope retrieval (BOND Epitope Retrieval Solution 1), stained with Anti-Ki67 (Cell Signaling cat# 12202S, 1:400) in combination with the BOND Polymer Refine HRP Plex Detection kit (Leica cat# DS9914), and counterstained with hematoxylin.

3. Results

Synthesis and characterization of 2155-14 and 2155-18. The pyrrolidine diketopiperazine compounds, 2155-14 (JC-395) and 2155-18 (JC-408), were synthesized by standard solid phase synthesis with MBHA resins. Amino acids were coupled to amine on the resin using Boc-AA-OH or

Preprints (www.preprints.org) | NOT PEER-REVIEWED | Posted: 15 May 2023 doi:10.20944/preprints202305.1006.v1

Fmoc-AA-OH (4 eq), HOBt (4 eq), and HATU (4 eq) in DMF containing 10% DIEA at 25 °C, and the Boc or Fmoc group was deprotected by 55% TFA in DCM or 20% piperidine in DMF at 25 °C, respectively. After coupling reactions with four amino acids and phenylacetic acid or 2-(adamantan-1-yl)acetic acid, five amide groups were reduced with borane in THF (~30 eq) at 70 °C under μwave irradiation for 6 hours. The reduced 2° amine groups were coupled with 1,1'-oxalyldiimidazole in anhydrous DMF, and diketopiperazine moieties were formed in the agent on the resin. TFA/TFMSA (9/1) was used to cleave the resin, and the final compounds were obtained by preparative HPLC purification with over 98% purity confirmed by the analytical LC. The structures of the final compounds were confirmed by ^{1}H NMR and Mass spectroscopic analysis, which were matched with the previous report (9).

In vivo efficacy study in A375 CDX. In the previous study we reported the lack of clinical and organ toxicity of 2155-14 and 2155-18 when tested at 50 mg/kg/day in Balb/C mice (10), which are immunocompetent. In the present study we utilize immunocompromised mice, therefore, we monitored for signs of clinical distress every day. As evidenced by Figure 1B, there was no overall weight loss as a result of the injections of the compounds. Additionally, all mice exhibited normal behavior suggesting the lack of distress.

A375 CDX was established by injection of A375 cells on day 9 after the arrival of mice. The tumors became palpable within two weeks after the injections. However, several mice did not develop tumors and were discarded from the study leaving 11 mice in each group. The tumors reached 100 mm^3 on day 29 after which we commenced the treatment. The efficacy of 2155-14 and 2155-18 became evident one week after the start of the treatment (Figure 2A). We continued the treatment for two weeks until the tumors of the vehicle control group reached maximum allowed volume, after which we discontinued the study. The tumor volumes of the treated groups were statistically significantly smaller than the vehicle control group throughout the entire study. On the final day of the study the tumor volume ratio between treated and vehicle control group reached 10-fold. To confirm this observation, we excised and weighed the tumors. As can be seen from Figure 2B, the weights of the tumors from the treated groups were statistically significantly smaller than the vehicle control group. Interestingly, three tumors from 2155-18-treated mice were not found upon necropsy, whereas all tumors from 2155-14-treated group were accounted for.

3.1. Figures, Tables and Schemes

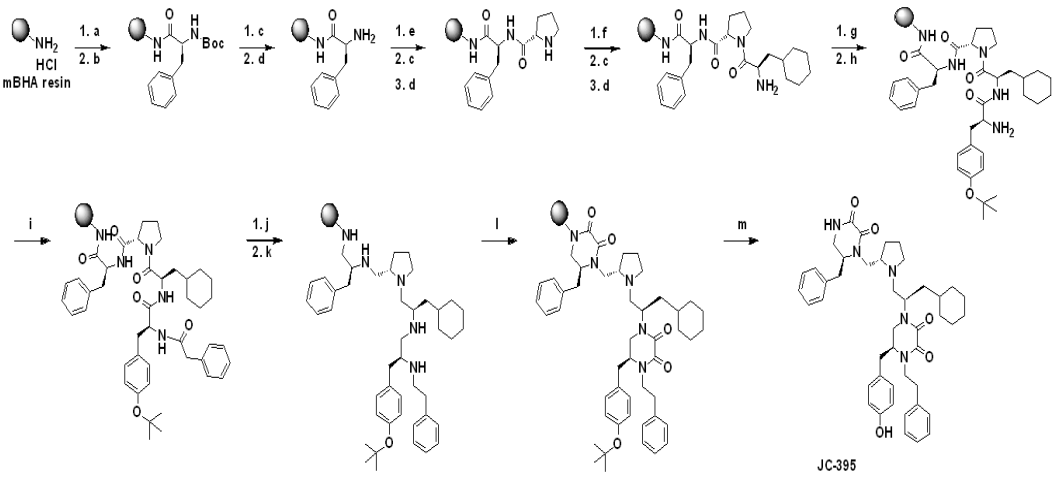

Scheme 1. Schemes for the synthesis of 2155-14 (JC-395) and 2155-18 (JC-408). Reagents and Conditions: a) 10% DIEA/DMF, 25 °C, 20 min; b) Boc-L-Phe-OH/HATU/HOBt (4 eq), 10% DIEA/DMF, 25 °C, 4 h; c) 55% TFA/DCM, 25 °C, 30 min; d) 10% DIEA/DCM 25 °C, 5 min (3x); e) Boc-L-Pro-OH/HATU/HOBt (4 eq), 10% DIEA/DMF, 25 °C, 2 h; f) Boc-β-cyclohexyl-D-alanine-OH/HATU/HOBt (4 eq), 10% DIEA/DMF, 25 °C, 2 h; g) Fmoc-L-Tyr (OtBu)-OH/HATU/HOBt (4 eq), 10% DIEA/DMF, 25 °C, 2 h; h) 20% Piperidine/DMF, 25 °C, 30 min; i) Phenylacetic acid/HATU/HOBt (4 eq), 10% DIEA/DMF, 25 °C, 2 h; j) Borane-THF, 70 °C (μwave), 6 h; k) Piperidine, 70 °C (μwave), 30 min; l) 1,1'-Oxalyldiimidazole (8 eq), DMF, 25 °C, 48 h; m) TFA/TFMSA (9/1), 25 °C, 1.5 h; Synthetic schemes for

Preprints (www.preprints.org) | NOT PEER-REVIEWED | Posted: 15 May 2023 doi:10.20944/preprints202305.1006.v1

JC-395 is present as a representative. For the synthesis of JC-408, the following conditions were applied: f) Boc-Phe-OH/HATU/HOBt (4 eq), 10% DIEA/DMF, 25 °C, 2 h; i) 2-(Adamantan-1-yl)acetic acid/HATU/HOBt (4 eq), 10% DIEA/DMF, 25 °C, 2 h.

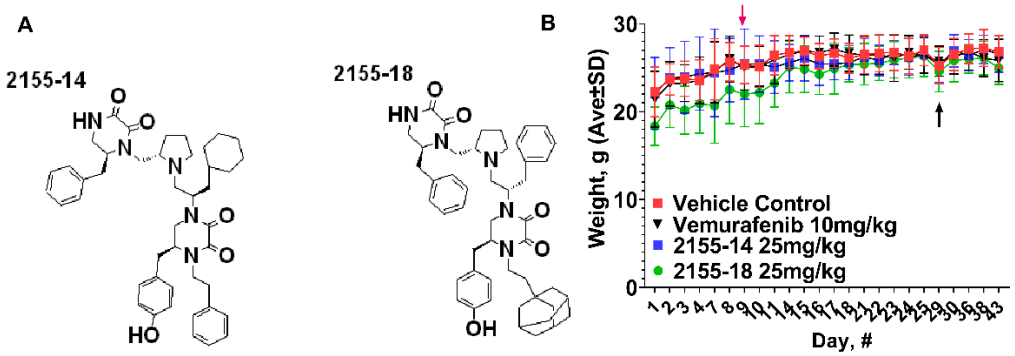

Figure 1. Structures and effect of 2155-14 and 2155-18 on nude mice body weight. Red arrow - day of A375 cell injection, black arrows - day of the first treatment.

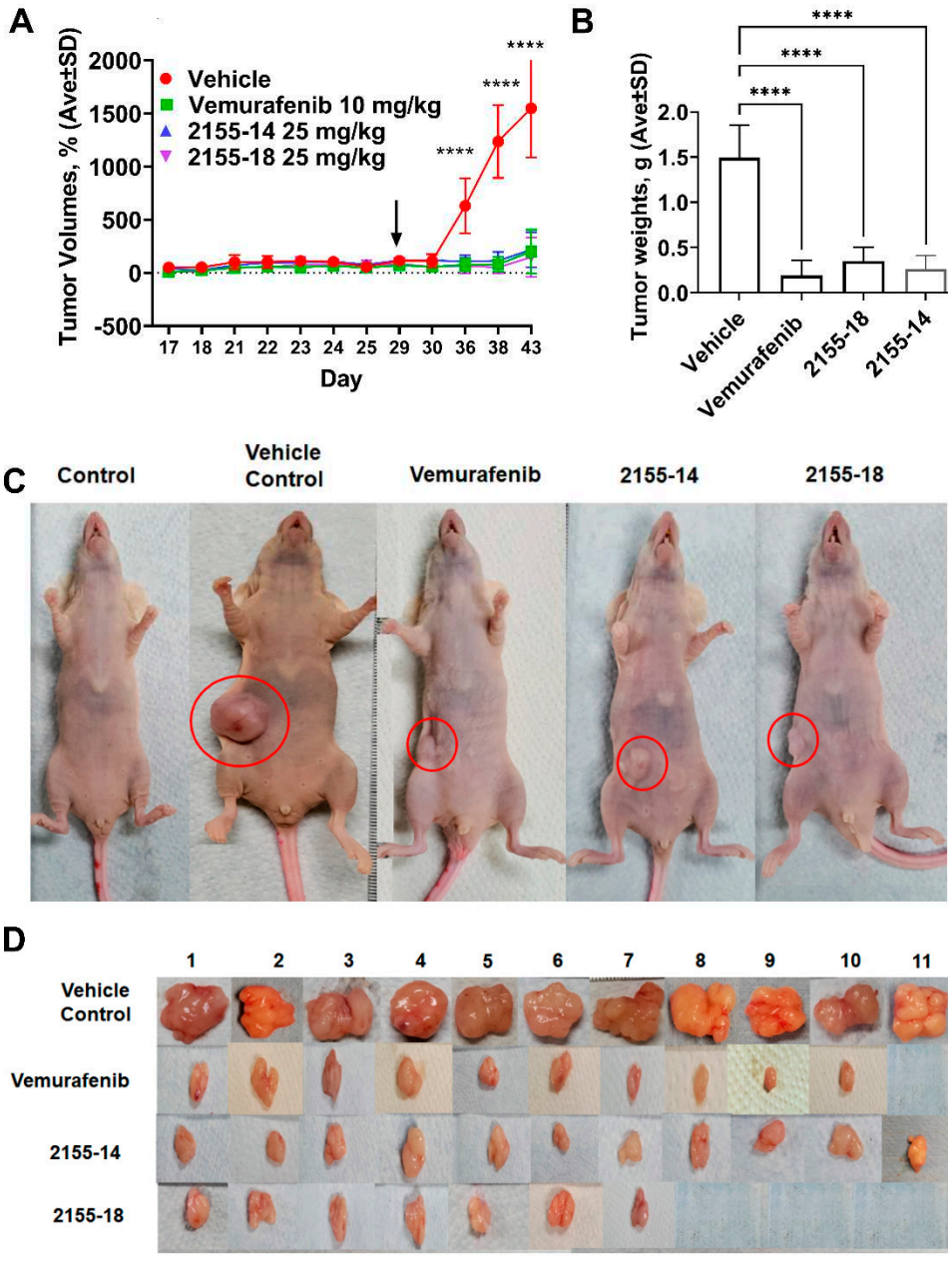

Preprints (www.preprints.org) | NOT PEER-REVIEWED | Posted: 15 May 2023 doi:10.20944/preprints202305.1006.v1

Figure 2. 2155-14 and 18 are efficacious in A375 CDX melanoma model. (A) Tumor volumes of mice treated with 2155-14 and 18 are significantly smaller than untreated control. (B) Weights of excised tumors confirm efficacy of leads. (C) Representative animals from each treatment group. (D) Excised tumors of treated animals are significantly smaller than of untreated control and, in some animals, undetectable. Red arrow - day of A375 cell injection, black arrows - day of the first treatment. **** - p-value < 0.0001 (n=11). The mice were allowed to acclimate after the delivery. Mice were treated three times per week using sub-cutaneous injections.

The excised tumors were stained for cleaved caspase 3 (CC3), an apoptosis marker, Ki67, a proliferation marker, and hnRNPH1/H2. Tumors treated with vemurafenib, 2155-14, and 2155-18 were positive for CC3 staining (Figure 3) consistent with their reported mechanism of cell death (8, 18). Tumors treated with 2155-14 and 2155-18 revealed decreased Ki67 staining similar to the tumors treated with vemurafenib, suggesting that cell proliferation is inhibited by the lead compounds (Figure 4).

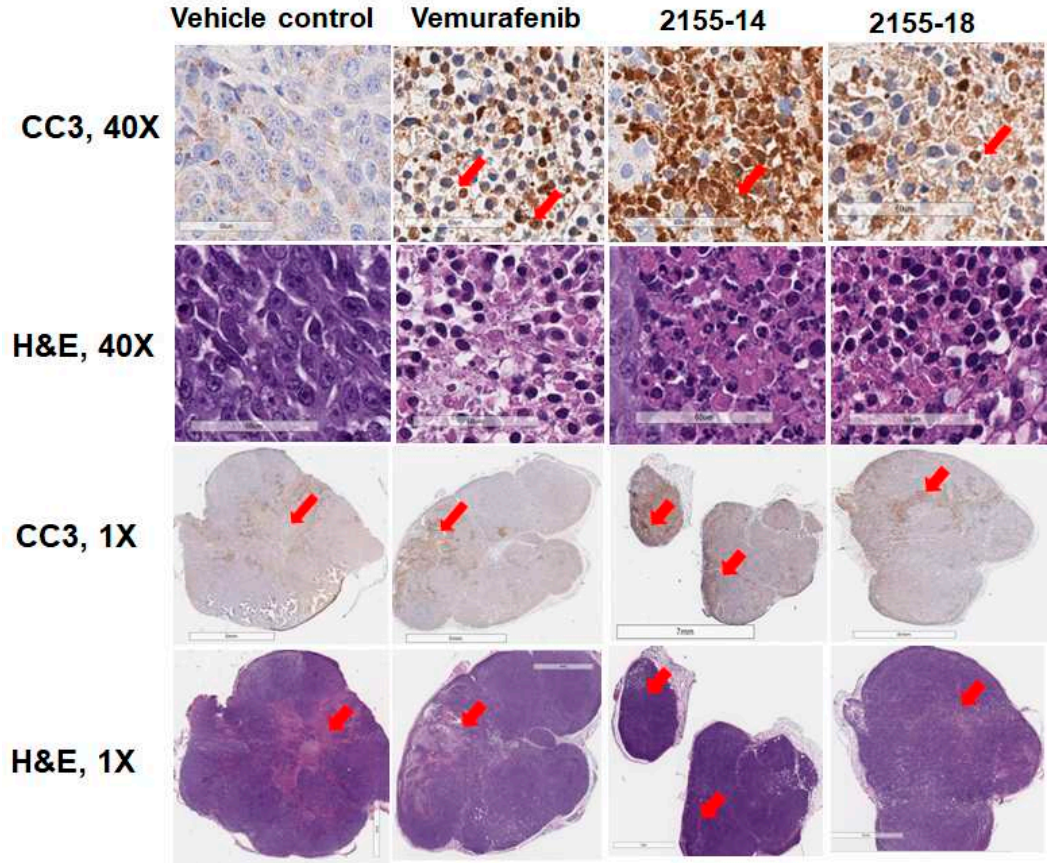

Figure 3. Immunohistochemical analysis of protein expression of cleaved caspase-3 in melanoma tumor sections (n = 3) indicates induction of apoptosis by 2155-14 and 2155-18. Images are captured by the Leica slide scanner, and representative images are shown. Scale bars for 40x images: 60 µm. Scale bars for 1x images: 7 mm. Red arrows in 40x images indicate examples of cells stained positive for CC3 (brown color). Red arrows in 1x images indicate areas stained positive for CC3 (brown color) and corresponding areas in H&E images.

Preprints (www.preprints.org) | NOT PEER-REVIEWED | Posted: 15 May 2023 doi:10.20944/preprints202305.1006.v1

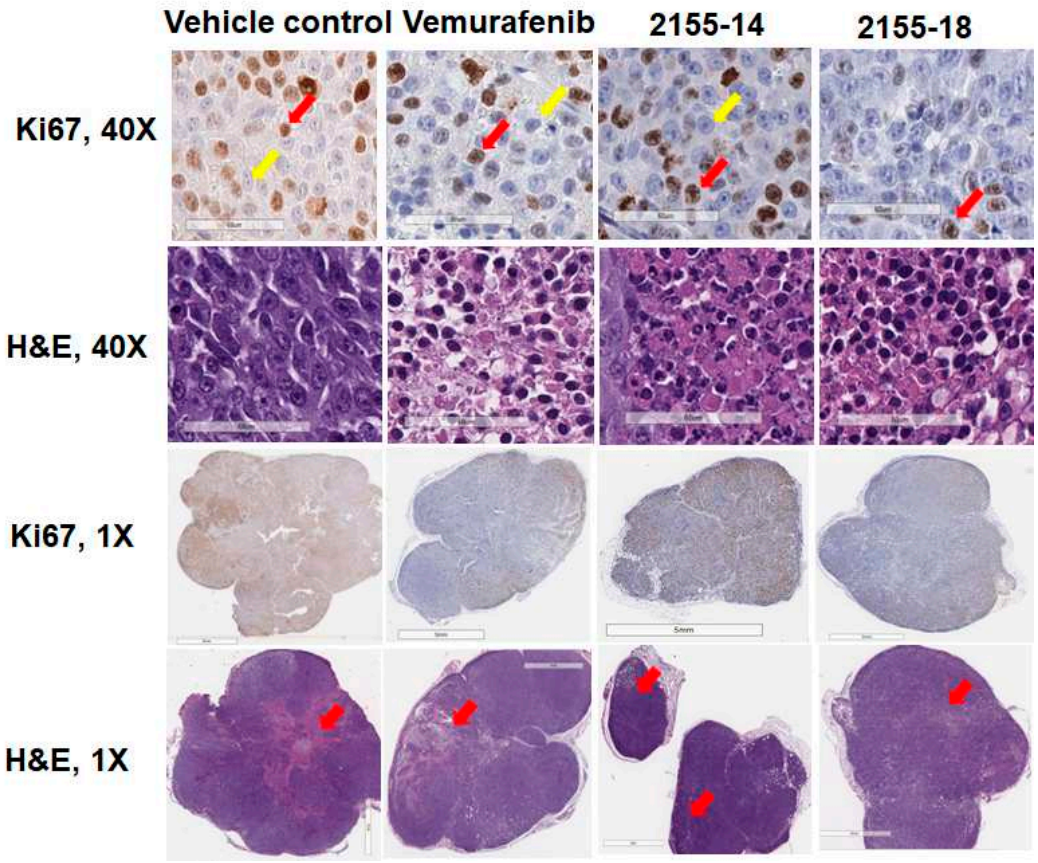

Figure 4. Immunohistochemical analysis of protein expression of Ki67 in melanoma tumor sections (n = 3) indicate inhibition of tumor proliferation by 2155-14 and 2155-18. Images are captured by the Leica slide scanner, and representative images are shown. Scale bars for 40x images: 60 μm. Scale bars for 1x images: 7 mm. Red and yellow arrows in 40x images indicate examples of cells stained positive and negative, respectively, for Ki67 (brown- or blue-stained nuclei, respectively). Red arrows in 1x H&E images indicate areas where apoptosis was detected by CC3 staining.

Preprints (www.preprints.org) | NOT PEER-REVIEWED | Posted: 15 May 2023 doi:10.20944/preprints202305.1006.v1

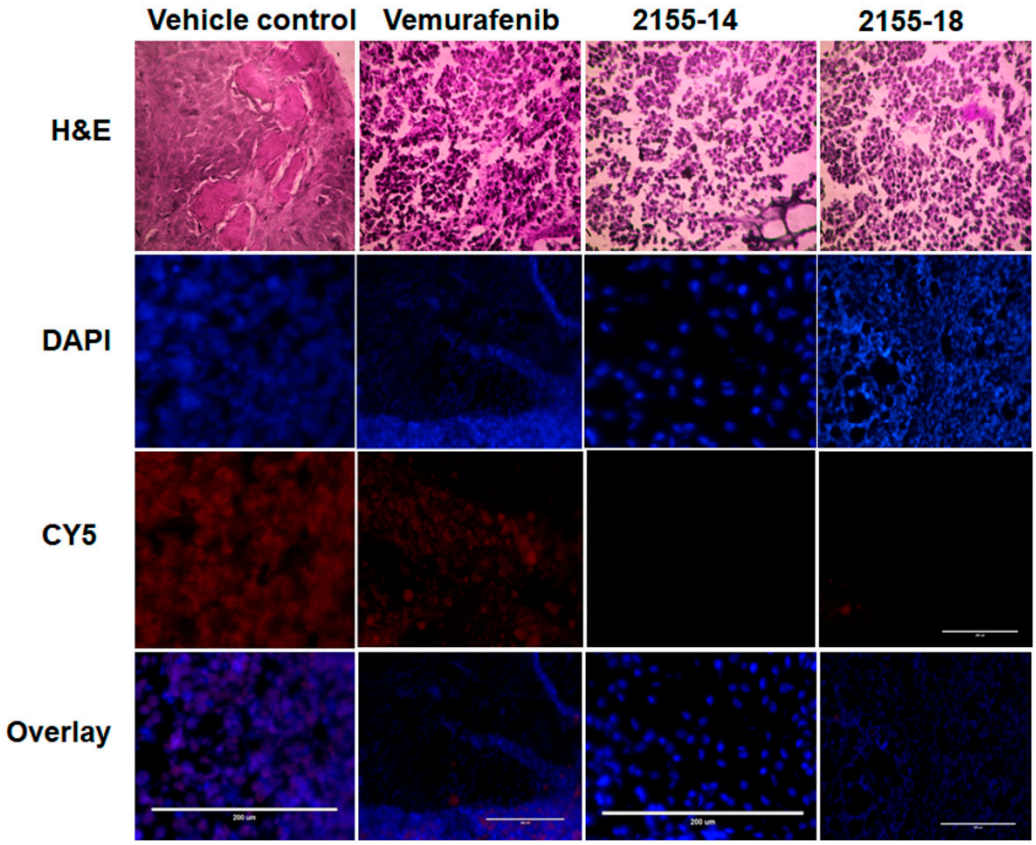

Figure 5. Immunofluorescence staining for hnRNP H1/H2 demonstrates its downregulation in tumors treated with 2155-14 and 2155-18 (n = 3). Images are captured by the Evos microscope, and representative images are shown. Note the lack of staining in the Cy5 channel corresponding to the lack of hnRNP H1/H2 protein expression in tumors treated with 2155-14 and 2155-18. Scale bars: 200 μm.

4. Discussion

The results presented in this study demonstrate efficacy of two novel anti-melanoma leads, 2155-14 and 2155-18, in A375 cell line-derived xenograft model. More specifically, the leads stopped tumor growth by blocking cell proliferation and caused apoptosis. To the best of our knowledge, this is the first example of compounds belonging to the pyrrolidine diketopiperazine chemotype demonstrating an anti-cancer activity.

Our group has previously shown that 2155-14 binds to spliceosomal proteins hnRNP H1 and H2 (8) causing ER stress and autophagy ultimately resulting in the apoptotic cell death. This is, to our knowledge, the first and so far, the only report of small molecules working via binding the above-mentioned molecular targets. hnRNP H1 and H2 are RNA-binding proteins involved in mRNA splicing, export, and stability in normal biology (19). Nothing is known about the role of hnRNPH1 and H2 in melanoma development and homeostasis. In other cancers, hnRNPH1 was shown to be upregulated in chronic myeloid leukemia (CML) patients and cell lines which correlated with disease progression (20). In the same study, in vivo and in vitro experiments showed that knockdown of hnRNP H1 inhibited cell proliferation and promoted cell apoptosis in CML cells. hnRNP H1 was also demonstrated to promote colorectal cancer progression via the stabilization of mRNA of Sphingosine-1-Phosphate Lyase 1 in vitro (21).

Mechanistically, the study by Uren et al., (22) identified a set of 1,086 high confidence target transcripts of hnRNP H1. Analysis of the target transcripts indicated that hnRNP H1's involvement in splicing is 2-fold: it directly affects a substantial number of splicing events, but also regulates the expression of major components of the splicing machinery and other RNA-binding proteins (RBPs) with known roles in splicing regulation. The identified mRNA targets displayed function enrichment

 doi:10.20944/preprints202305.1006.v1

in MAPK signaling and ubiquitin mediated proteolysis, which might be main routes by which H1 promotes tumorigenesis. However, this study was conducted in HeLa cells, and it is not clear whether hnRNP H1's role in melanoma cells is similar to its role in HeLa cervical carcinoma cells. Future studies will be directed at discerning the role of hnRNP H1 and H2 in melanoma.

5. Conclusions

The results of this study in combination with previous report (10) of lack of in vivo toxicity suggest that 2155-14 and 2155-18 can be used as drug development leads for melanoma therapy and in vivo and in vitro probes for melanoma research. Additionally, targeting hnRNP H1 and H2 represents a feasible approach to melanoma therapy.

Supplementary Materials: N/A

Author Contributions: DM and KSMS designed the study. DM obtained funding and wrote the manuscript. SV performed animal protocol, histology, and immunostaining, and co-wrote the manuscript. JZ performed histopathological evaluation of tumors and co-wrote the manuscript. JL and KS performed immunofluorescence studies. MB, BC, TS, and SD performed animal protocol. JYC co-wrote the manuscript, and AS and RS synthesized and characterized the compounds for the study.

Funding: This work was supported by NIH grant R15CA249788 (PI - DM). JYC and RS were supported by NIH SC2 award (SC2GM130470).

Institutional Review Board Statement: Animal experiments conform to internationally accepted standards and have been approved by the NSU IACUC.

Data Availability Statement: Not applicable.

Acknowledgments: N/A

Conflicts of Interest: The authors declare no conflict of interest.

References

1. Society AC. Key Statistics for Melanoma Skin Cancer2023. Available from: https://www.cancer.org/cancer/melanoma-skin-cancer/about/key-statistics.html.
2. Bomar L, Senithilnathan A, Ahn C. Systemic Therapies for Advanced Melanoma. Dermatol Clin. 2019;37(4):409-23.
3. C. Robert BK, J. Schachter, P. Rutkowski,, A. Mackiewicz DS, M. Lichinitser, R. Dummer,, F. Grange LM, V. Chiarion-Sileni, K. Drucis, I. Krajsova,, A. Hauschild BM, J. Legos, D. Schadendorf. Two Year Estimate of Overall Survival in COMBI-v, a Randomized, Open-Label, Phase III Study Comparing the Combination of Dabrafenib (D) and Trametinib (T) with Vemurafenib (Vem) as First-Line Therapy in Patients (Pts) with Unresectable or Metastatic. Eur J Cancer. 2015;51:s663.
4. Wolchok JD, Chiarion-Sileni V, Gonzalez R, Rutkowski P, Grob JJ, Cowey CL, et al. Overall Survival with Combined Nivolumab and Ipilimumab in Advanced Melanoma. N Engl J Med. 2017;377(14):1345-56.
5. Hodi FS, Chesney J, Pavlick AC, Robert C, Grossmann KF, McDermott DF, et al. Combined nivolumab and ipilimumab versus ipilimumab alone in patients with advanced melanoma: 2-year overall survival outcomes in a multicentre, randomised, controlled, phase 2 trial. The Lancet Oncology. 2016;17(11):1558-68.
6. Larkin J, Chiarion-Sileni V, Gonzalez R, Grob JJ, Cowey CL, Lao CD, et al. Combined Nivolumab and Ipilimumab or Monotherapy in Untreated Melanoma. New England Journal of Medicine. 2015;373(1):23-34.
7. Sharma P, Hu-Lieskovan S, Wargo JA, Ribas A. Primary, Adaptive, and Acquired Resistance to Cancer Immunotherapy. Cell. 2017;168(4):707-23.
8. Palrasu M, Knapinska AM, Diez J, Smith L, LaVoi T, Giulianotti M, et al. A Novel Probe for Spliceosomal Proteins that Induces Autophagy and Death of Melanoma Cells Reveals New Targets for Melanoma Drug Discovery. Cell Physiol Biochem. 2019;53(4):656-86.

9. Onwuha-Ekpete L, Tack L, Knapinska A, Smith L, Kaushik G, Lavoi T, et al. Novel pyrrolidine diketopiperazines selectively inhibit melanoma cells via induction of late-onset apoptosis. J Med Chem. 2014;57(4):1599-608.
10. Velayutham S, Seal T, Danthurthy S, Zaias J, Smalley KSM, Minond D. In Vivo Acute Toxicity Studies of Novel Anti-Melanoma Compounds Downregulators of hnRNPH1/H2. Biomolecules. 2023;13(2).
11. Penumutchu SR, Chiu LY, Meagher JL, Hansen AL, Stuckey JA, Tolbert BS. Differential Conformational Dynamics Encoded by the Linker between Quasi RNA Recognition Motifs of Heterogeneous Nuclear Ribonucleoprotein H. J Am Chem Soc. 2018;140(37):11661-73.
12. Bertoldo JB, Muller S, Huttelmaier S. RNA-binding proteins in cancer drug discovery. Drug Discov Today. 2023:103580.
13. Kuznetsov G, Xu Q, Rudolph-Owen L, Tendyke K, Liu J, Towle M, et al. Potent in vitro and in vivo anticancer activities of des-methyl, des-amino pateamine A, a synthetic analogue of marine natural product pateamine A. Mol Cancer Ther. 2009;8(5):1250-60.
14. Chen L, Aktas BH, Wang Y, He X, Sahoo R, Zhang N, et al. Tumor suppression by small molecule inhibitors of translation initiation. Oncotarget. 2012;3(8):869-81.
15. Eskens FA, Ramos FJ, Burger H, O'Brien JP, Piera A, de Jonge MJ, et al. Phase I pharmacokinetic and pharmacodynamic study of the first-in-class spliceosome inhibitor E7107 in patients with advanced solid tumors. Clin Cancer Res. 2013;19(22):6296-304.
16. Hong DS, Kurzrock R, Naing A, Wheler JJ, Falchook GS, Schiffman JS, et al. A phase I, open-label, single-arm, dose-escalation study of E7107, a precursor messenger ribonucleic acid (pre-mRNA) splicesome inhibitor administered intravenously on days 1 and 8 every 21 days to patients with solid tumors. Invest New Drugs. 2014;32(3):436-44.
17. Steensma DP, Wermke M, Klimek VM, Greenberg PL, Font P, Komrokji RS, et al. Phase I First-in-Human Dose Escalation Study of the oral SF3B1 modulator H3B-8800 in myeloid neoplasms. Leukemia. 2021;35(12):3542-50.
18. Beck D, Niessner H, Smalley KS, Flaherty K, Paraiso KH, Busch C, et al. Vemurafenib potently induces endoplasmic reticulum stress-mediated apoptosis in BRAFV600E melanoma cells. Sci Signal. 2013;6(260):ra7.
19. Geuens T, Bouhy D, Timmerman V. The hnRNP family: insights into their role in health and disease. Hum Genet. 2016;135(8):851-67.
20. Liu M, Yang L, Liu X, Nie Z, Zhang X, Lu Y, et al. HNRNPH1 Is a Novel Regulator Of Cellular Proliferation and Disease Progression in Chronic Myeloid Leukemia. Front Oncol. 2021;11:682859.
21. Takahashi K, Fujiya M, Konishi H, Murakami Y, Iwama T, Sasaki T, et al. Heterogenous Nuclear Ribonucleoprotein H1 Promotes Colorectal Cancer Progression through the Stabilization of mRNA of Sphingosine-1-Phosphate Lyase 1. Int J Mol Sci. 2020;21(12).
22. Uren PJ, Bahrami-Samani E, de Araujo PR, Vogel C, Qiao M, Burns SC, et al. High-throughput analyses of hnRNP H1 dissects its multi-functional aspect. RNA Biol. 2016;13(4):400-11.